

1

2

3 **Elevator Condition Monitoring: A Lightweight**
4 **Receptive Field and Temporal Correlations**
5 **Enhanced Deep Learning Model to Tackle**
6 **Imbalanced Dataset**

7

8

9

10

11

12

13

14

15

16

17

18

19

20

21

22

ABSTRACT

23

24 It has been witnessed with the thriving popularity of elevators in contemporary society during
25 modernization while posing an unavoidable challenge to consistently maintain their safety and
26 reliability in routine operations. The conventional monitoring mechanisms prove insufficient to
27 consistently monitor and evaluate the health condition of elevators in actual deployment. Under a
28 plethora of research utilizing data-driven approaches to measure the degradation status of elevators,
29 there also exist multiple industrial pain points while constraining their broad applications in the elevator
30 industry. For instance, the imbalanced dataset with rare abnormal samples in actual life would lead to
31 incomplete and inadequate representative feature learning during the model training process; the
32 excessive reliance on synthetic laboratory data with proprietary application domains in experiment
33 would impair the model's generalization capability; whilst the complex architecture as stacked in
34 pursuit of functionality comprehensiveness would by no means contribute to effectiveness enhancement
35 at the cost of efficiency decrease. This paper established a lightweight deep learning model with
36 streamlined elegant architecture to resolve the aforementioned issues. The real-life imbalanced data
37 have been collected and utilized directly under the devised algorithmic structure and training strategy
38 without any need for laboratory synthesis on their compositions, yet largely alleviating the impact of
39 imbalanced dataset phenomenon in effect. With the proposed effective feature extraction mechanisms,
40 the receptive field and temporal correlations have been enhanced to further facilitate the monitoring
41 efficiency and accuracy. As validated by the systematic experimental results, the receptive fields have
42 been enlarged by 75% in comparison with the vanilla model structure and the parameter quantity have
43 also been reduced by 21% while boosting the model's training and inferencing efficiency during the
44 actual deployment. Meanwhile, in order to rigorously evaluate the model's robustness, the results have
45 been thoroughly validated after splitting the dataset for multiple times with comprehensive ablation
46 study scenarios to explore the optimal model configuration parameters. The proposed model
47 demonstrated its superior performance by the outstripped average detection precision ratios under
48 asymmetrical data allocations while shedding light on its practical application by industrial practitioners
49 for real-life elevator condition monitoring.

50

51

52 *Keywords* — Anomaly detection, condition monitoring, deep learning, elevator system, Internet of
53 Things (IoT), real-observed dataset

54

Managerial Relevance Statement

55
56
57
58
59
60
61
62
63
64
65
66
67
68
69
70
71
72
73
74
75
76
77
78
79
80
81
82
83
84
85
86
87
88
89
90
91

This paper conducts innovative research with feasible data-driven solutions to facilitate the condition monitoring capability on elevators in actual life, which sheds light on the managerial decision-making in adoption of such deep learning-oriented data-driven methods during the real elevator operation process for engineering managers and policy makers. As well acknowledged that there exist considerable deficiencies by the conventional way of monitoring for elevator anomaly detection, which might cause unavoidable latencies or induce hazardous accidents. By the prevailing condition monitoring practice, such existing issues as the imbalanced dataset, architectural complexity and insufficient feature extraction have impaired the generalization capability of deep learning models in their applications to the elevator condition monitoring domain. This paper proposes a lightweight streamlined deep learning model to boost the condition monitoring effectiveness on elevators without exerting additional computational burden, which could be broadly applied based on the real-life imbalanced dataset without the need for excessive data manipulation or feature engineering. Overall speaking, the important managerial insights can also be summarized from the following three-layer statement: 1). Problem Layer: There exist deficiencies and shortcomings in the conventional way of elevator condition monitoring mechanisms, whilst likely to induce hazardous events during the elevator operation process; 2). Solution Layer: The proposed lightweight deep learning model can effectively resolve the existing issues while improving the elevator condition monitoring efficiency and tackling the imbalanced dataset issue; 3). Deliverable Layer: By enhancing the temporal feature correlations with enlarged receptive fields, the proposed data-driven approach achieves superior performance compared with prevailing baseline models, while shedding light on the utilization of feasible AI solutions for elevator condition monitoring with improved monitoring efficiency and effectiveness. Concretely speaking, through the smart monitoring of elevators by the proposed solution, the elevator's safety and reliability shall be leveraged on a large scale, which is crucial for assisting the engineering managers in elevator manufacturing and maintaining enterprises to improve their working efficiency and effectiveness. Meanwhile, the adoption of such a data-driven approach for elevator condition monitoring also sheds light on the execution of practical ways with the employment of artificial intelligence in the safety-critical domains, while enlightening the policy makers in the relevant government bureaus in enacting the relevant guidelines for regulating the utilization of AI in elevator-relevant safety domains. The proposed solution shall assist the engineering managers and policy makers to help with their strategic decision making while embracing the artificial intelligence-oriented digital transformation technologies, thus providing a meaningful and impactful solution to enhance the elevator safety monitoring efficiency and effectiveness for practical applications during the elevator modernization process. Additionally, the captioned study shall contribute to a couple of SDGs: SDG 9 and SDG 11, while fostering sustainable industrialization with technological innovation with more resilient and reliable infrastructure under the Smart City as facilitated.

92 1. Introduction

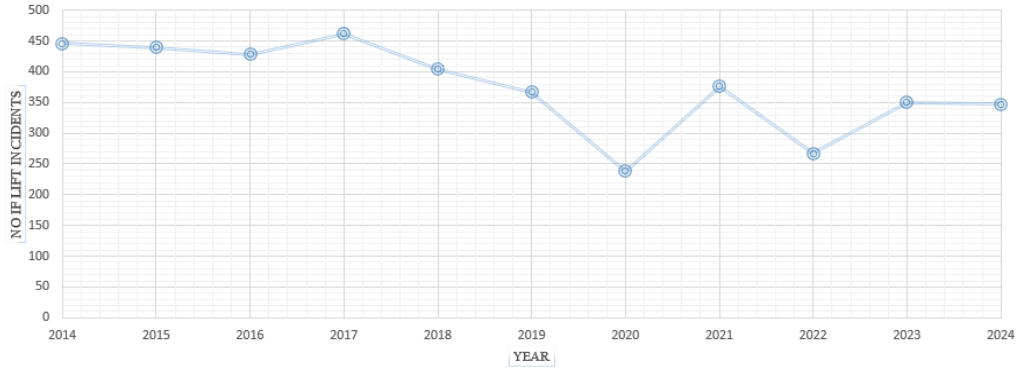
93 With the thriving development of technology and rapid improvement of living standards, people put
94 much more emphasis than ever on the reliability and safety of their routinely used instruments and
95 apparatus, including elevators assimilated into people's everyday life in metropolitan areas.
96 Consequently, how to enable the smart monitoring of elevator conditions by the adoption of cutting-edge
97 deep learning algorithms to integrate the non-invasive Internet-of-things (IoT) (Aheleroff et al., 2020;
98 Wang et al., 2021) sensors under Industry 4.0 (Giovanni et al., 2024) with real-life data collection has
99 become a top concern for academia and industrial practitioners during the digital transformation process
100 (Gao et al., 2025; Lakemond et al., 2024).

101 The elevator (or referred as "Lift" in this paper), as an indispensable part of contemporary society,
102 plays an irreplaceable role in ensuring the convenient haulage and smooth transportation of goods and
103 passengers. With the increasingly extensive utilization of lift systems in commercial skyscrapers,
104 residential mansions, industrial facilities, and office buildings, it demands high-level attentive
105 maintenance for elevators to ensure the safety of pedestrians and passengers. However, it is discovered
106 that most lift accidents are incurred by the mechanical pitfalls or the degradation of lift components that
107 probably being installed decades ago, while posing great challenges for the lift registered contractors
108 (RC) to conduct the systematic modernization in prevention of hazardous events. According to the latest
109 statistics as released by the Hong Kong Electrical and Mechanical Services Department (EMSD) in Fig. 1,
110 there were totally 375 reported lift accidents during 2021, in comparison of 367 reported accidents in
111 2019 and 238 accidental events as recorded in 2020 (EMSD, 2022c). Such accidents come thick and fast
112 consecutively each year, hence it proves imperative for lift RCs to abide by the compulsory requirement
113 with effective condition monitoring to ensure the reliability of lift systems. In order to optimize the
114 existing situation with safety assurance and risk mitigation, EMSD has launched the "Lift and Escalators
115 Ordinance (Chapter 618)" (EMSD, 2022b) and "Code of Practice (CoP)" (EMSD, 2022a) with concrete
116 measures and statutory requirements as legislated to regulate the lift construction and maintenance work.

117 Nevertheless, in view of the complexity of elevator systems, the existing industrial practice proves
118 insufficient to ensure the smooth operation of lifts with hazard prevention. The maintenance work is
119 normally conducted either periodically or after the failure of lift systems with passive condition
120 evaluation and excessive overheads. The prevailing countermeasures are mainly focused on the
121 installation of destructive transducers interlinking the subcomponents with the speed encoder,
122 weighbridge, and other relevant components. Despite of the professionalism and expert knowledge
123 (Xiahou et al., 2021) needed for installation of such intrusive sensors, the maintenance also demands the
124 service interruption with repetitive data analysis and extra workmanship for condition evaluation through
125 the specialized equipment and proprietary software designed under a specific lift brand.

126

127
128
129
130
131
132



133
134

Fig. 1. The recorded elevator incidents in Hong Kong during the past 10 years (EMSD, 2025)

135
136
137
138
139
140
141
142
143
144

Embraced by technological advancement, there are also emerging trends for installing non-intrusive sensors (de Oliveira et al., 2022) with collaborative maintenance (García et al., 2022) in combination with conventional monitoring manners. Meanwhile, more industrial practitioners and academia are investigating the possibility for non-intrusive elevator condition monitoring by the adoption of data-driven oriented artificial intelligence (*AI*) (Medghalchi & Vogel, 2024; Xu & Lin, 2025; Yu et al., 2024) without interference on the intrinsic circuitry of elevators. Whereas there exist industrial bottlenecks for mass implementation after consulting the domain experts in lift industry: (i) lack of abundant real abnormal data and real-observed dataset; (ii) lack of effective AI model for adoption in such safety critical systems; (iii) lack of the holistic framework with the integration of non-invasive IoT sensors (Rajnoha & Hadač, 2024) for condition monitoring of complex systems in real applications.

145
146
147
148
149
150
151
152
153

In order to fundamentally tackle the aforementioned problems, we established a deep learning (DL) oriented data-driven approach to construct the smart condition monitoring system for elevators (Mishra & Huhtala, 2019). By means of the well-established model, no sophisticated feature engineering needed, while the multivariant current signals as abstracted via non-invasive sensors were fed into the architecture with automated feature extraction and real-time anomaly detection. By the proposed model architecture, the receptive fields have been enlarged dramatically with enhanced temporal correlations, which could leverage the feature extraction capability of the DL model in tackling the real-case data patterns during elevator condition monitoring process after commissioning. The main contributions are listed in the following:

154
155
156

i) Establish the holistic elevator condition monitoring framework that integrates a deep learning-based health index predictor and an anomaly detector, tailored for application on non-intrusive one-dimensional sensor signals.

157
158
159

ii) Propose the state-of-the-art deep learning-based model comprising a one-dimensional dilated convolutional neural network (1D-Dilated CNN) with expanded receptive fields, followed by a concatenated gated recurrent unit (GRU) architecture to further fetch the temporal correlations within

160 the multi-variant data, while enhancing the feature extraction capability for efficient elevator condition
161 monitoring.

162 iii) Propel the theoretical advancement with the proposed model architecture to tackle the imbalanced
163 dataset during the elevator condition monitoring process in real life by creatively designing the devised
164 training strategy and loss function.

165 iv) Construct the real-world elevator condition monitoring dataset reflecting actual multi-variant data
166 patterns under the realistic industrial operating conditions and validate the model robustness with
167 multiple dataset splitting through the systematic ablation study.

168 The remainder of this paper is organized as follows: Section 2 briefly overviews the prevailing
169 methods for condition monitoring of E&M systems; Section 3 formulates the problem with the defined
170 objective function; Section 4 illustrates the architecture of the established 1D-DiCNN-GRU DL model;
171 Section 5 introduces the data pre-processing procedure with data concatenation and segmentation
172 process; Section 6 demonstrates the experiment results after splitting the dataset and Section 7
173 concludes this paper with a brief summary.

174 **2. Related works**

175 **2.1 Conventional Ways of Elevator Condition Monitoring**

176 Condition monitoring for the electrical and mechanical (E&M) system has been conducted with
177 plethora of research focusing on the conventional approaches with physics-guided or knowledge-based
178 empirical methods for anomaly detection based on embedded sensors (Dai & Gao, 2013; Khan et al.,
179 2024; Yin et al., 2014). The Physics of Failure (PoF) approach has been integrated into reliability
180 engineering for complex systems as evolved with significant attention on the prediction accuracy
181 amongst environmental and operational influential factors (Zeng et al., 2016). Generally speaking, PoF
182 method has been regarded as one of the conventional but invaluable techniques that being widely
183 utilized for prevention of failure occurrence while encompassing the intricate practices of reliability
184 design in mechanical systems (Wileman et al., 2021). As for the model-based methods that proposed in
185 (Esteban et al., 2014), they devised the approach for detecting the anomalies of E&M sub-systems while
186 employing the Linear Parameter Varying (LPV) model for joint estimation on the elevator performance.
187 As explored by (González et al., 2019), the model-based approach for evaluating the guiding rails was
188 utilized in the vertical transportation systems with extended Kalman filter (EKF) for quantitative
189 diagnosis. However, both the conventional PoF method and model-based method would require the
190 prior predecessor knowledge about the mechanical condition or maintenance histories about a specific
191 brand of elevator with process mining (Tang et al., 2023) to investigate the root causes against the
192 system failures. Nevertheless, such previous experience or prior knowledge proved difficult to acquire

193 across different brands of elevators, which posed the restriction for application with such vanilla
194 methods in real practice especially under the Industry 4.0 processes (Mazzoleni et al., 2022).

195 **2.2 Emerging Trends of Elevator Condition Monitoring with Machine Learning Approaches**

196 In view of the aforementioned shortcomings, there has been an emerging approach with AI-based
197 (Koutsoupakis et al., 2023) or specifically machine learning (ML)-based (Arora et al., 2022) data-driven
198 methods that has given rise across different industrial domains (Hennig et al., 2021; Kumar Sharma et
199 al., 2022; Moura et al., 2019). Some previous work was focused on the variants of support vector
200 machines (SVM) to diagnose the vibration signals from the elevator doors for detecting the
201 malfunctioning components using the least squared SVM (LS-SVM) (Wan et al., 2015). Under the
202 complex mechanical system of elevators, there emerged another approach with fault detection based on
203 Bayesian network algorithm for the motor, gearbox, brake, sheave, suspension rope and lift car (Liu et
204 al., 2017). Under the fusion approach, the model combining the particle swarm optimization (PSO)
205 algorithm and back propagation (BP) neural network were employed for lift door fault prediction and
206 diagnosis (Wen et al., 2016). Whereas the mentioned approaches inevitably need the redundant process
207 for feature engineering in order to delineate the feature profiles and inter-dependencies, thus burdening
208 the computation complexity with unnecessary offloading, especially under the multi-variant high-
209 dimensional dataset (Fu et al., 2021).

210 **2.3 IoT Integrated Monitoring with Deep Learning Methods**

211 Some of the latest studies investigated the installation of IoT sensor nodes (Ilango et al., 2022; Skog
212 et al., 2017) to build the Internet-of-Elevators with non-invasive fault monitoring. For instance, the
213 work as mentioned in (Chai et al., 2021) employed the architecture with long short-term memory
214 (LSTM) and convolutional neural network (CNN) model for extracting the temporal and spatial
215 correlations. Whereas the paper failed to address the imbalanced dataset problem, and the proposed
216 model demonstrated complex architecture with excessive parameters.

217 To further streamline the DL model with reduced parameters, the dilated CNN model architecture
218 was initially proposed by (Koltun, 2016), mainly utilized in semantic segmentation, natural language
219 processing (NLP) and computer vision (CV) relevant domains. The notable improvement of Dilated
220 CNN in comparison with conventional CNN architecture lies in its architecture with the devised dilated
221 rate to enlarge the receptive field without adding additional model parameters, nor expanding the kernel
222 size (Li et al., 2023; Xu et al., 2022). The Gated Recurrent Unit (GRU) architecture was proposed in
223 (Chung, 2014), the invention of which was to remedy the vanishing gradient issues encountered with
224 LSTM model with streamlined architecture. By reducing the original three gates of LSTM to the two
225 gates in GRU, namely the “update gate” and “reset gate”, it is validated that the learnable parameters
226 and kernel computations are dramatically reduced without performance deprivation to enhance the
227 efficiency.

228 Despite the work conducted by predecessors with fault diagnosis of industrial processes and
229 machinery (Feng et al., 2021; Yan et al., 2022), the systematic research for elevator health monitoring
230 (Chen et al., 2021) via IoT sensor nodes using the advanced DL methods has been scarcely conducted
231 (Nguyen et al., 2022). Moreover, from the perspective of data-driven approaches with AI utilization for
232 Human-Machine Collaboration (HMC) (Lingxiao et al., 2025), it has been discovered that in the domain
233 of elevator condition monitoring, the previous work is either reliant on the synthetic laboratory data or
234 seldomly focused on the feasible solutions to tackle the real-life imbalanced dataset issue, which is quite
235 commonly encountered in real syndromic surveillance of elevators during actual operations.

236 **2.4 Attempts in Tackling Imbalanced Dataset and Limitations for the Problem Domain**

237 Under the scope of DL for alleviating the impact of imbalanced datasets, there exist previous
238 research works attempting to adopt measures from different aspects aiming to leverage fault diagnosis
239 accuracy. For instance, there exists the One-class Classification (OCC) algorithm to address the limited
240 data sample issues in distributed systems (Lin et al., 2018). Thereafter as a typical example, the one-
241 class SVM-based fault diagnosis method was explored based on the feature space-located distance
242 metrics (Mahadevan & Shah, 2009). Whereas such methods would be overshadowed by complex
243 datasets, especially when extracting the dominant features from the elevator's heterogeneous multi-
244 variant real-monitoring data. In the presence of sample generation techniques, there also exist shallow
245 oversampling algorithms such as ADASYN (Haibo et al., 2008), SMOTE (Huo et al., 2015), Geometric
246 SMOTE (Douzas & Bacao, 2019), Random-SMOTE (Dong & Wang, 2011) etc. By adding the
247 synthesized minority class of samples, though such methods could help alleviate the asymmetry data
248 allocation issues, the generated instances might fail to represent the underlying density against the
249 elevator's dynamic operation environment during the synthesization process, thus falling into the
250 overlapping noisy areas and weakening the actual performance (Analide et al., 2020). Similar to the
251 principle for data augmentation, the latest generative AI (GAI) technology has given rise to the
252 utilization of deep generative models (DGM) (Tomczak, 2024) in domains of CV and semantic
253 segmentation etc. However, in its adaptation to industrial applications for 1D data facilitation, the
254 current literature has scarcely been covered. Meanwhile, the training complexity of DGM might impact
255 the inferencing efficiency for real-time monitoring during the actual operation process. The evaluation
256 metrics against the generated anomalous samples with appropriate manifestations remain insufficiently
257 explored while arousing hesitation from industrial practitioners for practical deployment.

258 **2.5 Niche Statement**

259 The prevailing industrialized approaches are mainly focused on the utilization of conventional
260 physics-guided empirical methods while lacking the generalization capability across the diversified
261 application scenarios. Whilst the ML-based methods cannot alleviate the redundant process for feature
262 engineering with the burdened computational complexity. Regarding the DL-integrated data-driven

263 approach with real-case IoT sensor nodes, it is discovered that seldom research has entered such a sphere
264 in actual operation, while mainly relying on synthetic laboratory data for analysis. Despite of efforts
265 devoted to tackling the imbalanced dataset issue, there exists a lack of feasible methods for real-life
266 adoption during the elevator's real operation process. It thus requests the model with high inferencing
267 efficiency applicable to real-time monitoring scenarios, without a complex algorithmic structure nor
268 overshadowed performance against the multi-variant accumulative data during the elevator's routine
269 monitoring process, which becomes the research niche of our work. Hence under such conditions, in
270 the domain of elevator condition monitoring, how to design a feasible and executable DL model with
271 leveraged efficiency while tackling the imbalanced dataset issue with a devised lightweight but elegant
272 architecture for real-case efficient application could be a worthwhile direction carried with valuable
273 research impacts.

274 **3. Problem formulation**

275 **3.1. Holistic elevator condition monitoring framework**

276 By the hierarchical design, there are four primary non-intrusive IoT sensors installed to extract the
277 current signals from the core components of the elevator, namely the traction motor, brake, safety circuit
278 and lift door (as shown in Fig. 2). The holistic framework is composed of multiple IoT sensor nodes for
279 real-life data acquisition without intervening the normal operation process of the elevator. The devised
280 DL model is employed for real-time fault detection and prognostics with broad application potential
281 during the elevator modernization or retrofitting process. The workflow is summarized by below stages:

282 Stage 1). Data capturing and acquisition. The non-intrusive clamp-type current sensors are installed
283 to fetch the electric current signals flowing through the core components during real-life observation.

284 Stage 2). Data transference and storage. The micro-controller is configured with Raspberry Pi 4i for
285 data transfer under 4G LTE router and upload to the cloud-based data storage hub empowered by
286 Amazon Web Services (AWS).

287 Stage 3). Data analysis and anomaly detection. The DL-based model is employed to analyse the real-
288 life data with condition monitoring and health status evaluation. The anomaly detection results will be
289 provided to the lift maintenance crew to support the predictive maintenance (Jaenal et al., 2024) with
290 prognostic health management (PHM).

291 **3.2. Monitored components**

292 The measured components are explicitly demonstrated in Fig. 3, with electric current signature
293 analysis for real-time condition monitoring. The distance sensor and reflection plate are installed with
294 the aim of capturing the distance between the roof of elevator car and the ceiling of shaft for velocity
295 calculation.

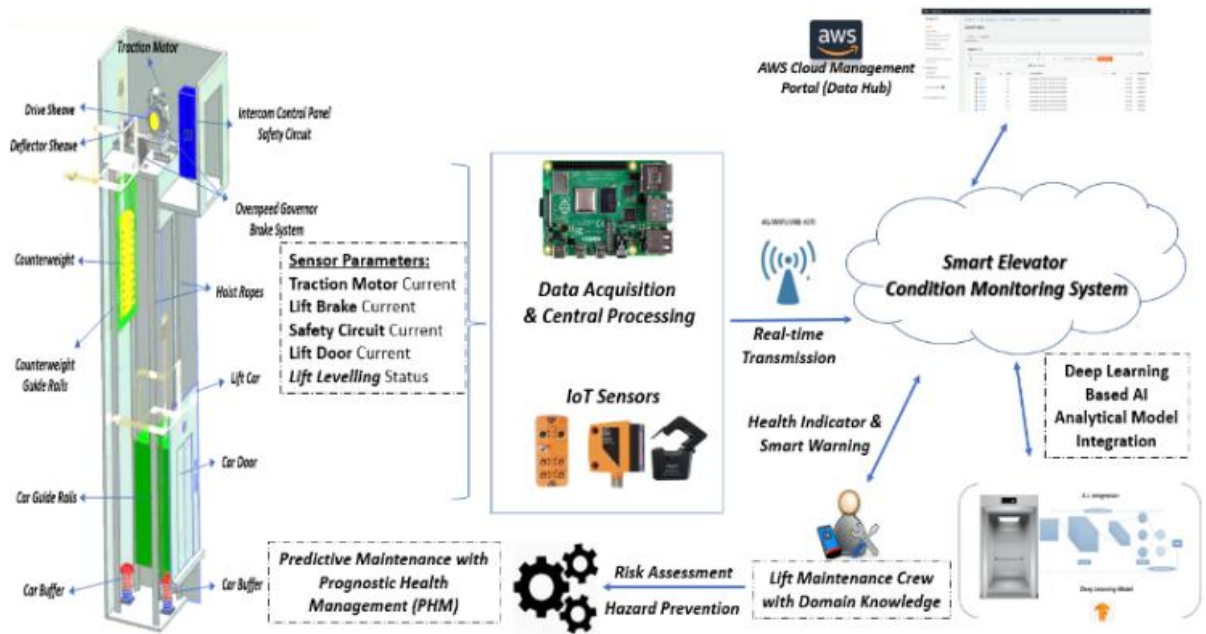


Fig. 2. Overview of the non-intrusive smart elevator condition monitoring framework.

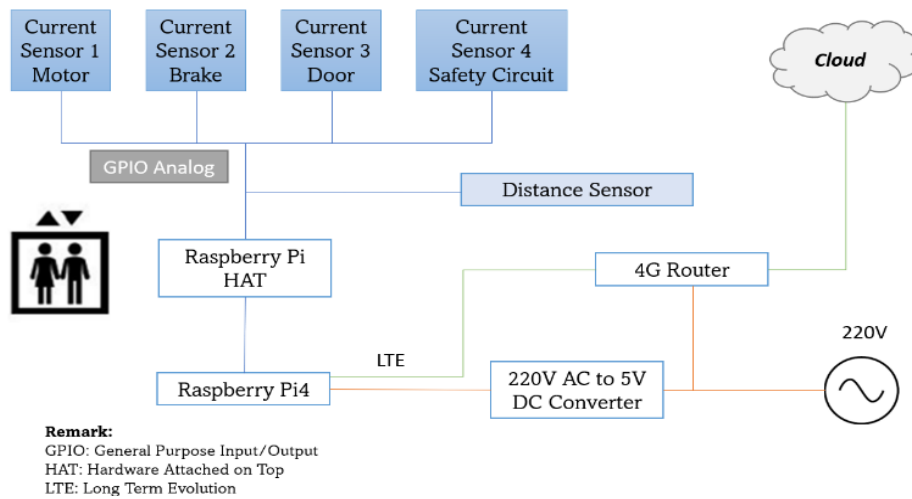


Fig. 3. Overview of the monitored components.

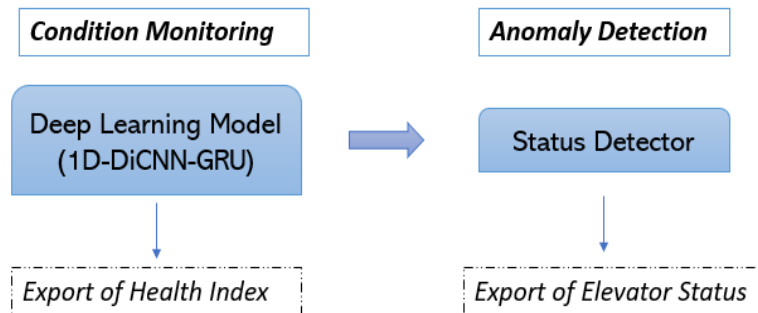


Fig. 4. Workflow components of the proposed model framework.

313 1) *Traction Motor*

314 The asynchronous AC (alternating current) motors are widely equipped on elevators to empower the
315 magnetic ropes with driving force. The magnetic and electric circuits are interlinked with the inner
316 components as the stator and rotor, generating the electromagnetic induction to convert into mechanical
317 energy. Hence the electric current signals passing through the motor is one of the critical factors to
318 ensure the haulage and kinetic power supply for the elevators.

319 2) *Brake*

320 The elevator is normally equipped with the magnetic power-off brake system. The brake coil shall
321 be demagnetized when lift is halted with the power supply being cut off. The pressure plate and cover
322 plate are forced by the tensioned springs to get the friction disc tightly locked, while impeding the
323 rotation of hub and shaft to stop the elevator.

324 3) *Safety Circuit*

325 The safety circuit acts as the core component interlinking the safety relays with hazards prevention
326 by lift notch-off, while reducing the risk to the acceptable level.

327 4) *Door*

328 The door of elevator serves as the indispensable part to ensure the safe travel of passengers. The lift
329 door motor is energized to open and close the lift gates shortly after the lift parked at the designated
330 floor with consecutive spikes of door current, acting as the indicator to reflect the lift motion.

331 **3.3. Problem statement**

332 Under the holistic condition monitoring framework as illustrated, it has been recognized as the
333 industrial bottleneck encountered with imbalanced dataset during lift observation. Hence the aim of this
334 paper is to devise an elegant DL model to analyse such multi-variant signals from the four measured
335 components with imbalanced dataset, in the aim of monitoring the condition of elevators with anomaly
336 detection (Fang et al., 2023).

337 Let X_{im} be the input of multi-variant electric current signals under real-life imbalanced dataset with
338 $X_{im}=\{x_1, x_2, x_3, x_4\}$ (Ahelerooff et al., 2020) and let $Y_h=\{1,0\}$ be the health index reflecting the status of
339 elevator, where Y_h equals “1” means the elevator in good health condition.

340 Under the task of condition monitoring with estimation on the elevator’s health condition, our aim is
341 to minimize the variation between the predicted health index and the true condition of elevators as
342 interpreted by the overall objective function depicted in the following equation:

343
$$\min_{\theta} \|f_D(X_{im}; \theta) - Y_h\|, \quad (1)$$

344 where f_D denotes the lightweight DL network with learnable parameter Θ , Y_h represents the elevator's
 345 health index. The objective is to minimize the difference and deviation between the predicted health
 346 index and the actual health condition of elevators under the heterogeneous imbalanced data distribution,
 347 such that the situation of elevators could be determined with enhanced accuracy and efficiency,

348 **4. Model architecture**

349 In this section, we shall give a detailed introduction to the DL solution for the problem stated in
 350 *Section 3*. The proposed DL framework is elaborated with the framework (as shown in Fig. 4 comprising
 351 of two parts. One is the one-dimensional stacked dilated convolutional neural network (1D-Dilated CNN)
 352 followed by a GRU regression head (1D-DiCNN-GRU) for the task of condition monitoring; the other
 353 as the “status detector” with binary classification to determine whether any anomaly is detected based
 354 on the health index value as output from the previous part.

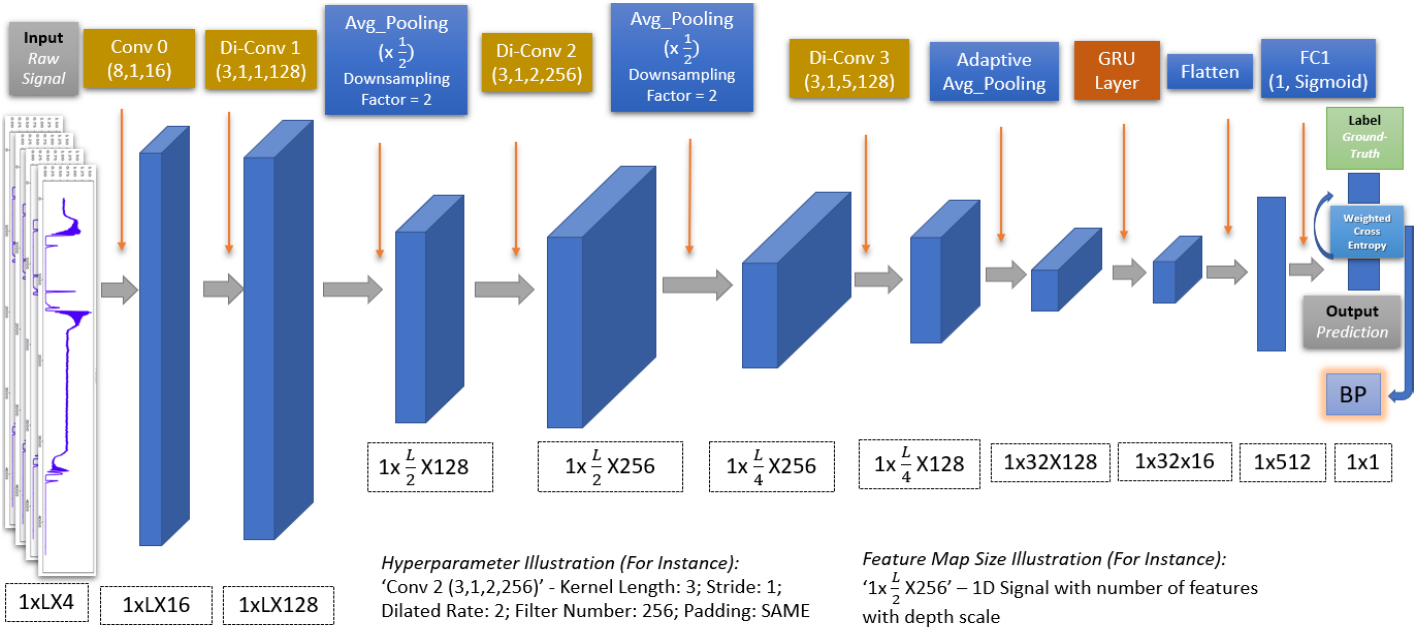
355 **4.1. 1D-DiCNN-GRU model**

356 As shown in Fig. 5, the model basically consists of a series of vanilla or dilated 1D convolutional
 357 layers, and a GRU. More specifically, in this paper, the multi-variant 1D signal will first go through a
 358 vanilla 1D convolutional layer with kernel size equal to “8”, and then pass a cascade of three stacked 1D
 359 dilated convolutional layers with the same kernel size 3 but different dilated rates – “1, 2, 5”, respectively.
 360 We set the dilated rates as “1, 2, 5” sequentially, so as to exponentially expand the receptive field without
 361 loss of any coverage, in other words, getting rid of the gridding effect with minimized artifacts caused
 362 by the dilated convolution. This combined dilation rates configuration can ensure a dense and contiguous
 363 coverage span traversing the input data, which also helps the model better capture the long-term
 364 dependencies existing in the elevator's real-monitoring data.

365 Among the three stacked 1D dilated convolutional layers with kernel size of “3”, assume that there
 366 are M filters with input dimension as “ $1 \times N$ ”, the feature map in the l -th layer can be represented by
 367 Equation (2).

$$368 \quad 369 \quad x_j^l = f\left(\sum_{i=1, \dots, N} x_i^{l-1} \times k_{ij}^l + b_j^l\right), j = 1, \dots, M \quad (2)$$

370 where f denotes the activation functions with x representing the convolutional operations; x_i^{l-1} and x_j^l
 371 denote the l -th input feature map and the output map on the j -th layer; k_{ij}^l and b_j^l denote the kernel and
 372 the corresponding bias of the j -th layer respectively.



373

Fig. 5. Workflow components of the proposed model framework.

374

375

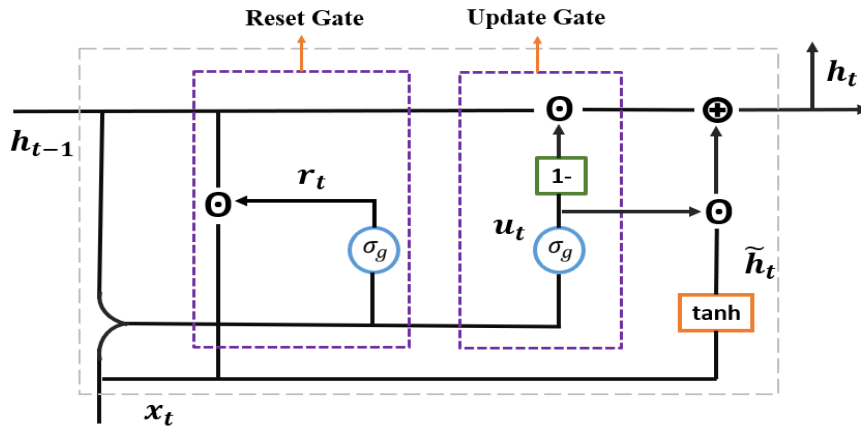
376

377

378

379

380



381

Fig. 6. GRU cell structure as concatenated in the proposed model.

382

383

384

385

386

387

388

389

390

391

It should be noted that an additional vanilla convolutional layer with large kernel size “8” is added before the three dilated convolutional layers to further enhance the capability of the network to investigate temporal correlation within the input signal at low level. It is very crucial to enlarge the receptive field of the neuron, especially for our case as the input sequence is extremely long, containing thousands of timestamps. The temporal correlation between far neighbors will not be grasped if the receptive field is not big enough. And the proposed combination of one vanilla convolutional layer and three stacked dilated convolutional layers can take care of this issue effectively with less parameters compared to the scenario with all vanilla convolutional layers. Out of the four convolutional layers is the feature of size “ $I \times L/8 \times 128$ ”. An adaptive average pooling layer is then applied to uniform the length of the extracted feature as “32”.

392 As the convolutional kernel will slide towards one direction only, from left to right, for example, in
 393 the 1D convolutional layer, the feature we obtained after the adaptive average pooling layer basically
 394 remains the chronological order as the raw input. Based on this characteristic, on top of the CNN module
 395 we adopt a GRU (as shown in Fig. 6) to capture the inherent temporal correlation within extracted
 396 features and then fully connect to the final output, instead of using the trivial multilayer perceptron (MLP)
 397 model (Bisong, 2019) as the regression head. Experiments in *Section 6* proved the superiority of our
 398 proposed network.

399 The operation inside of GRU cell can be depicted by following formula:

$$400 \quad u_t = \sigma_g(W_{zx}x_t + W_{zh}h_{t-1}) \quad (3)$$

$$401 \quad r_t = \sigma_g(W_{rx}x_t + W_{rh}h_{t-1}) \quad (4)$$

$$402 \quad \tilde{h}_t = \tanh(Wx_t + r_t \odot W_{hh}h_{t-1}) \quad (5)$$

$$403 \quad h_t = (1 - u_t) \odot \tilde{h} + u_t \odot h_{t-1} \quad (6)$$

404 where u_t denotes the update gate, r_t represents the reset gate, \tilde{h}_t describes the candidate state of the
 405 hidden node, h_t represents current hidden state and h_{t-1} denotes the previous hidden state; x_t is the
 406 model input and W is the weight matrices; \odot denotes the element-wise dot product, whilst σ_g and \tanh
 407 denote the Sigmoid and tanh activation functions respectively.

408 The 1D-DiCNN-GRU model takes the regression task with estimated health index valued between
 409 “0” and “1” as the output. Based on the health index, the second part of framework serves as the anomaly
 410 detector to do the conditional classification to determine whether the lift system is in good condition or
 411 not by comparing the predicted health index to the anomalous threshold.

412 **4.2. Characteristics of adaptive pooling layer**

413 The devised 1D-Dilated CNN backbone includes three stacked blocks composed of one 1D-Dilated
 414 convolutional layer and an average pooling. With the aim to reduce the feature dimensions, pooling
 415 layers are critical to alleviate computational complexity. Considering the multi-variant signals in
 416 different lengths under multi-instance learning (MIL) (Liu et al., 2021), the adaptive pooling was
 417 utilized to trim and standardize the signal length to “32” before fed into the GRU. Below equation
 418 demonstrated the operation of the pooling layer with feature map calculation for the l -th layer.

$$419 \quad x_j^l = f(\beta_j^l \mathcal{D}(x_j^{l-1}) + b_j^l), j = 1, \dots, M \quad (7)$$

420 where M denoted the number of maps, f stands for the activation function and \mathcal{D} represents the pooling
 421 (down-sampling) function; β_j^l and b_j^l denote the bias for multiplication and addition accordingly of the
 422 j -th filter, while x_j^l & x_j^{l-1} stand for the output and input maps of the j -th filter after and before the
 423 pooling operation.

424 The adaptive pooling layer as concatenated before the GRU ensures the uniform length of input for
 425 the last fully connected layer. Consequently, the model is capable of processing the arbitrary length of
 426 signals for inference. It is the adaptive selection of kernel size that enables the adaptive pooling layer to
 427 produce outputs with same length regardless of the input length of raw signals to accommodate our
 428 application scenarios with lift condition monitoring.

429 **4.3. Employment of weighted cross entropy loss**

430 It has been one of the primary goals to tackle the imbalanced dataset of lift while lacking abnormal
 431 data (Zhou et al., 2021). The countermeasures proposed by this paper are categorized into two approaches,
 432 namely the devised training strategy and the refined loss function.

433 The loss function was employed in light of cross-entropy that being utilized to measure the difference
 434 between two probability distributions as follows,

$$435 \quad H(q,p) = - \sum_{x \in \chi} q(x) \log(p(x)) , \quad (8)$$

436 where q and p represent sample distribution of the ground truth and prediction respectively, χ represents
 437 the support. To further tackle the problem with imbalanced dataset to improve the convergence speed
 438 and training accuracy during evaluation, we have come up with the weighted cross entropy as for
 439 weighting the loss function to achieve the optimal balance with improved performance. The
 440 corresponding formula as obtained by Equation (3).

$$441 \quad H(q,p) = - \sum_{x \in \chi} \omega(x) q(x) \log(p(x)) , \quad (9)$$

442 where $\omega(\cdot)$ is the weight function. Particularly, in this paper, $q = \{y, 1 - y\}$, $p = \{\hat{y}, 1 - \hat{y}\}$, and the
 443 loss function can be rewritten as follows explicitly,

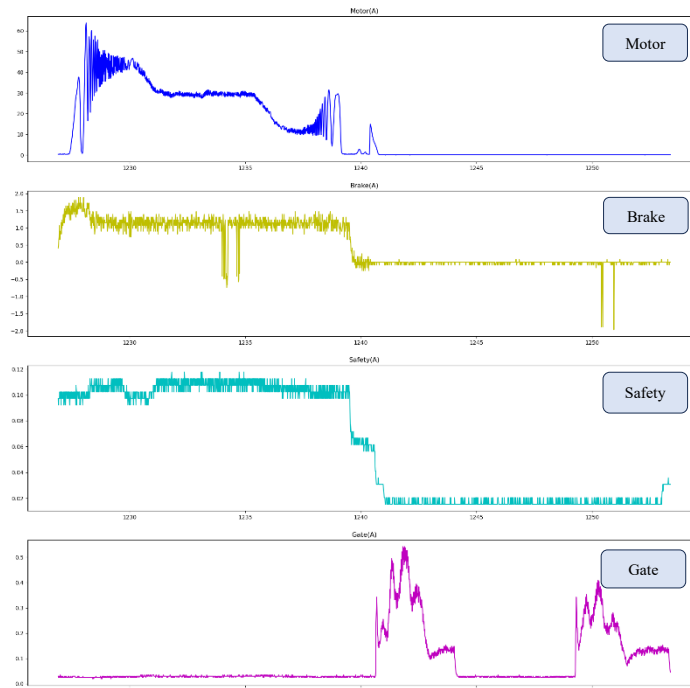
$$444 \quad L_{\theta} = -\omega \cdot y \log \hat{y} - (1 - y) \log (1 - \hat{y}) , \quad (10)$$

445 where $\hat{y} = f_D(X; \theta)$, and ω denotes the loss weight.

446 The ablation study was conducted accordingly in *Section 6 – Experiments*, while further discussing
 447 how the weight selection could affect the testing results. The optimum weight was selected afterwards
 448 to adjust and balance the portion of normal and abnormal dataset. By the refined allocation, the weighted
 449 cross entropy loss function as affiliated with MLP dense layer could help tackle the issue under
 450 imbalanced dataset. The trend of the exported mean absolute error (MAE) values was observed so as to
 451 continuously monitor the elevator’s health condition and to strategically integrate with the anomaly
 452 detector for consecutive status evaluation.

453 **5. Data preprocessing**

454 In this section, the data preprocessing details are provided with elaboration on the data concatenation
 455 and segmentation mechanism for training sample generation.



456 **Fig. 7.** A typical cycle with homogeneous segmentation.

457 The real data were collected from a lift with model of EXDN/VVVF as manufactured by “Fujitech”,
 458 which was installed at one of routinely used office buildings in Hong Kong. Specifically, the four multi-
 459 variant current signals were collected during the period from 1 Nov 2020 till 31 Dec 2020 with sampling
 460 frequency of 70 Hz. All collected data have been pre-processed with totally 39367 segments prepared.

461 **5.1. Velocity calculation**

462 The increase and decrease of the monitored distance indicate the motion of lift in descending and
 463 ascending status. Generally, the fluctuation on distance and velocity are compared with the current
 464 variations of two consecutive timestamps to determine the lift movement with predefined threshold as
 465 encoded in our algorithm. The aim of the calculation is to capture the starting and ending point for the
 466 lift movement as reflected in the levelling/velocity variations, while further discovering the correlations
 467 with multi-variant current data.

468 **5.2. Data homogeneous segmentation**

469 For explicit display of the multi-variant current signals to discover their correlations, the input signals
 470 were partitioned into a set of homogeneous operational segments. Each segment starts when the velocity
 471 variations were detected at the initiation point and ended when the elevator halted, followed by two
 472 consecutive spikes of door current, while indicating the open and closure of elevator gates for passenger
 473 offboarding and onboarding.

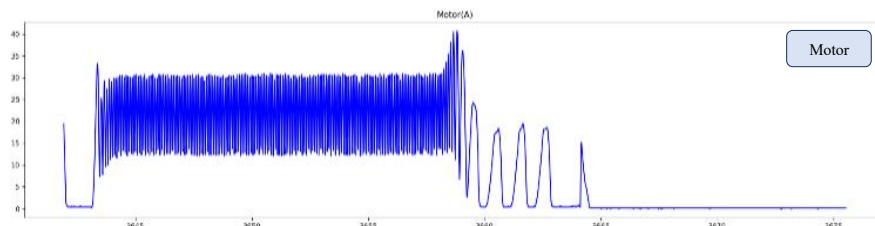
474

475

476

477

478



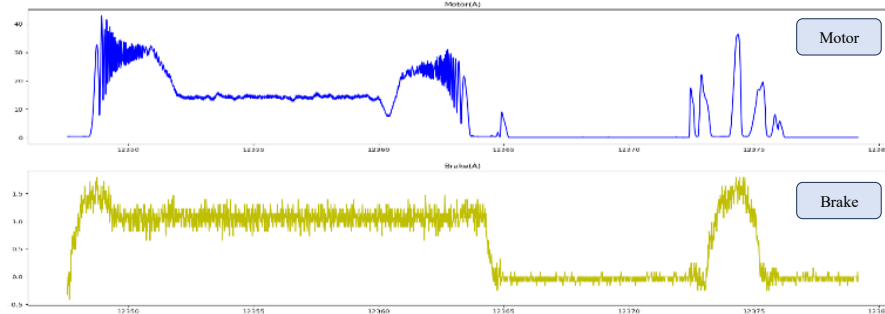
479

Fig. 8. Observed abnormal pattern with condensed waveform for traction motor.

480

481

482



483

484

Fig. 9. Observed abnormal pattern with abrupt current increase.

485

486

487

488

489

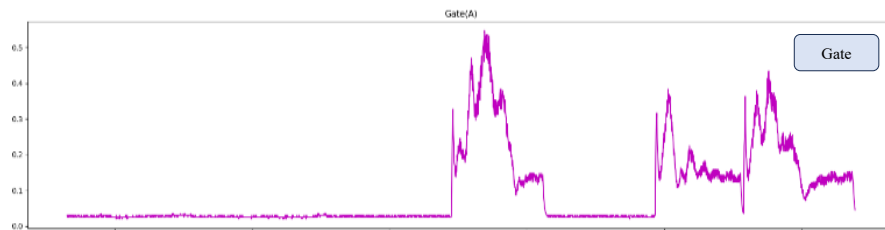


Fig. 10. Observed abnormal pattern with door closing issue.

491

The concatenated data were processed with automated homogeneous segmentation while including *i)* elevator car motion and *ii)* door motion (open and close). The normal patterns of current signals of the four measured components within a typical lift movement cycle were depicted by Fig. 7.

494 5.3. Observation of abnormal sequence patterns

495

During the data pre-processing process, we discovered three characteristics of the potential anomalies as reflected in the current patterns of the traction motor, brake and the lift door as elaborated respectively in the following section.

498 1) Condensed Motor Current

499

The induction motor is functioned to drive the magnetic rope with haulage and kinetic energy. The normal motor current starts with peak spike waveform at initialization to empower the lift car while triggering the sub-peak when prepared for a halt at certain floors. During the observation, the condensed waveform pattern of motor current was discovered in Fig. 8. Under advice from the domain experts, one of the potential root causes might be related with the gradual degradation of traction motor, as located in rotor bar or shaft, that inducing more current drawn.

504

505 **Table 1.**
506 Number of samples preparation in dataset.

Dataset	Sequence Quantity	Normal Condition	Abnormal Condition
Training	8049	7896	153
Validation	1012	996	16
Test	1023	1008	15

507 2) *Abrupt Surging of Motor & Brake Current*

508 The electric current flowing through the brake and traction motor shall be synergized to power the
509 lift car with movement. This abnormal situation was observed via the pattern of unstable current signals
510 with abrupt increasement as shown in Fig. 9, which could be induced by the potential degradation of
511 subcomponents in the brake. Under ruffle effect, the conjunct motor current also increased simultaneously
512 thus indicating the needs for comprehensive checking with status evaluation.

513 3) *Door Closing Issues*

514 The lift door anomalies occurred when odd number of consecutive spikes of current signals were
515 spotted. As shown in Fig. 10, the detected three spikes of gate current indicated an additional third gate
516 motion after opening/closure. As discussed with domain experts, it might be induced by the
517 malfunctioning of door sensor or obstruction on the trackway, with the gate bounced back in consecutive
518 movements.

519 **6. Experiments**

520 In this section, the training strategy and model hyperparameters shall be introduced and justified
521 accordingly, together with the anomaly detection threshold and evaluation metrics configuration. Under
522 *Subsection 6.2*, the systematic *Ablation Study* shall be conducted while exploring and substantiating the
523 model concatenation rationale, the loss function design and the batch size selection. The model
524 compression experiment results and performance benchmark against other state-of-the-art baseline
525 models shall be conducted as well with results unveiled since *Table 4* till *Table 6* after splitting the dataset
526 multiple times for objective comparison. The model's efficiency and convergence performance were
527 validated as well thereafter.

528 As illustrated in *Section 5*, the whole dataset as prepared incorporates 10084 multivariant signals with
529 three types of abnormal samples acquired through real observation. From the dataset summary as listed
530 in Table 1, the allocation for training dataset, validation dataset and testing dataset takes around 8:1:1
531 under appropriate proportion. The experiment was carried out via computer with Max. 5.1 GHz 8-core
532 i7 10875H CPU (16GB RAM), equipped under Nvidia GeForce GTX-2060 GPU using TensorFlow
533 framework in Python 3.6.

534

535

536 **Table 2.**
537 Details of dilated CNN+GRU.

Conv 0 (8,1,16)	
<i>Kernel Size:</i> 8; <i>Stride:</i> 1; <i>Padding:</i> Same (Same input and output length)	538
<i>Filter Number:</i> 16 (16 Kernels with length as L)	
Conv 0 Output: $1 * L * 16$ (Feature Map Size)	539
Dilated Conv 1 (3,1,1,128)	
<i>Kernel Size:</i> 3; <i>Stride:</i> 1; <i>Dilated Rate:</i> 1; <i>Filter Number:</i> 128 (128 Kernels with length as L)	540
<i>Padding:</i> Same	
Dilated Conv 1 Output: $1 * L/2 * 128$ (Feature Map Size)	541
Avg Pooling with <i>Down-sample factor:</i> 2; Length turned to $L/2$.	
Dilated Conv 2 (3,1,2,256)	542
Increased dilated rate to 2 for larger receptive field.	
<i>Padding:</i> Same	543
Dilated Conv 2 Output: $1 * L/4 * 256$ (Feature Map Size)	
Avg Pooling with <i>Down-sample factor:</i> 2; Length reduced to $L/4$.	544
Dilated Conv 1 (3,1,5,128)	
Increased dilated rate to 5 for larger receptive field.	
<i>Padding:</i> Same	545
Dilated Conv 3 Output: $1 * L/8 * 128$ (Feature Map Size)	
Adaptive Avg Pooling: Uniform the length of the output of previous dilated conv layer to 32.	546
Adaptive Avg Pooling Output: $1 * 32 * 128$ (Feature Map Size)	
GRU cell (16)	547
Number of hidden neurons in the gate: 16	
GRU cell output: $1 * 32 * 16$ (Feature Map Size)	548
FC1 (1, Sigmoid): Fully Connected Layer with predicted health index (predicted label).	
FC1 Output: $1 * 1$.	549

550

551 **Table 3**
552 Details of vanilla CNN+MLP

Conv 1 (8,1,128)	553
<i>Kernel Size:</i> 8; <i>Stride:</i> 1; <i>Padding:</i> Same (Same input and output length)	
<i>Filter Number:</i> 128 (128 Kernels with length as L)	554
Conv 1 Output: $1 * L/2 * 128$ (Feature Map Size)	
Avg Pooling with <i>Down-sample factor:</i> 2; Length turned to $L/2$.	555
Conv 2 (5,1,256)	
Reduced Kernel Size with <i>deepened</i> filter (filter number added to 256)	
Conv 2 Output: $1 * L/2 * 256$ (Feature Map Size)	556
Avg Pooling with <i>Down-sample factor:</i> 2; Length reduced to $L/4$.	
Conv 3 (3,1,128)	557
Reduced Kernel Size with <i>less deepened</i> filter (number reduced to 128)	
Conv 3 Output: $1 * L/2 * 128$ (Feature Map Size)	558
Adaptive Avg Pooling: Uniform the length with 32 extracted features.	
Depth GAP: Global Average Pooling through depth as reduced to 1.	559
Depth GAP Output: $1 * 32$	
FC1 (32, ReLU): Fully Connected Layer with input and output with 32 neurons.	560
Activation function: ReLU.	
FC1 Output: $1 * 32$.	561
FC2 (1, Sigmoid): Fully Connected Layer with predicted health index (predicted label).	
FC2 Output: $1 * 1$.	562

563

564

565 6.1. Training strategy and model hyperparameter

566 During the training process, with the aim of balancing the normal and abnormal data allocation to deal
567 with the imbalanced dataset issue, it was particularly configured with the devised algorithm to force the
568 allocation of abnormal data (negative data) with “1/8 portion” among the data in each mini batch. For
569 instance, the batch size was set as “8”, among which there were 7 normal samples with one abnormal
570 sample. The model hyperparameters are outlined in Table 2 with batch size of “8” over 100 epochs in
571 Adam optimizer and “1.00e-4” learning rate.

572 6.1.1 Anomaly detection threshold selection

573 The back propagation (BP) is conducted to consecutively update the parameters with iterations and
574 export the predicted health index value (with Sigmoid activation), as represented by $h(x)$ in Equation
575 (11).

$$576 f(x) = \begin{cases} normal, & h(x) > \lambda \\ anomaly, & h(x) \leq \lambda \end{cases} \quad (11)$$

577
578 The anomaly detection classifier is illustrated with λ as the threshold, the value of which has been
579 acquired while traversing all the samples in validation dataset with the best performance. According to
580 our experiment, the optimal threshold λ was acquired with the value as “0.8”. Consequently, when $h(x) >$
581 “0.8”, the system was determined as healthy; when $h(x) \leq$ “0.8”, the condition was judged as abnormal
582 with anomaly detected.

583 6.1.2 Evaluation metrics

584 The overall results were further examined via below metric by the “Precision” score, “Recall” score
585 and the “F1-Score” accordingly since Equation (12) till Equation (14) for performance evaluation.

$$586 \text{Precision} = \frac{\text{TruePositive (TP)}}{\text{TruePositive (TP)} + \text{FalsePositive (FP)}} \quad (12)$$

$$587 \text{Recall} = \frac{\text{TruePositive (TP)}}{\text{TruePositive (TP)} + \text{FalseNegative (FN)}} \quad (13)$$

$$588 \text{F1-Score} = 2 * \frac{\text{Precision} * \text{Recall}}{\text{Precision} + \text{Recall}} \quad (14)$$

589 The confusion matrix was employed to measure the overall performance. Except for the critical FP
590 ratio that we were intended to reduce, the FN condition should also be one of the consideration factors
591 in order to improve the maintenance efficiency to avoid the laborious attentive operations with extra
592 unnecessary field checking especially when confronted with shortage of elevator technicians.

593 6.2. Ablation study

594 A series of experiments have been conducted to get the final 1D-DiCNN-GRU model as specified in
595 Table 2. In this section, we shall analyze all the experimental results in detail, showing advantages of

596 each component in the model, while verifying the effectiveness of the training strategy described in
597 Section 6.2.

598 Specifically, the capability of dilated CNN feature extractor followed by the GRU regression head
599 will be addressed through the comparison with the vanilla CNN-MLP framework. And then the selection
600 of hyperparameters such as the loss weight in weighted binary cross entropy loss, and the batch size for
601 training would be investigated. Two approaches to reduce the number of parameters of the network and
602 strengthen potential generalizability of the model were studied, and we finally concluded with our
603 proposed model in Table 2 and Table 3. In order to enhance the rigorousness of the proposed model for
604 comprehensive validation, we have split the dataset and summarized the representative results after
605 splitting and testing multiple times. Afterwards, the averaged performance for anomaly detection was
606 evaluated via two metrics, namely the mean value - *Ab. M.* (μ) and standard deviation value - *Ab. S.* (σ)
607 correspondingly. The results were shown in Table 4, Table 5 and Table 6 accordingly to justify the model
608 concatenation and hyperparameter selection configurations.

609 **6.2.1 Reason for dilated CNN in concatenation with GRU**

610 In this section, we compared the model performance between the proposed model to the vanilla CNN-
611 MLP framework as described in Table 3. From the collection of confusion metrics results in Table 4 after
612 splitting the dataset, it was found that the dilated CNN + GRU (32) performed the best with mean values
613 (μ) of Precision/Recall and F1-Score reaching the highest standard deviation (σ) as the least after splitting
614 the dataset. The model performance could be qualitatively evaluated as well by analysing the confusion
615 matrix results. Compared to the best model dilated CNN + GRU (32), by replacing the dilated CNN
616 feature extractor with the vanilla CNN, more defects were not identified with smaller mean and larger
617 deviations on average. Likewise, by substituting the GRU with the trivial MLP, some normal samples
618 were mis-classified as anomalous, which also demonstrated the suboptimal performance in comparison.
619 As a result, the dilated CNN+GRU shows stronger capability in extracting features and capturing their
620 internal temporal correlation.

621 **6.2.2 Reason for weighted binary cross entropy loss function**

622 In order to alleviate the influence of imbalanced dataset, we have applied weighted cross entropy
623 (WCE) as the loss function for training. As the ablation study, we selected different weights ω imposed
624 on the normal samples to test the model performance. When the weight $\omega < "1"$, one can expect that
625 less attention will be paid to the normal samples, and in turn, more will be exerted on the contribution of
626 abnormal samples to the final loss. While $\omega = "1"$ means that no extra attention is paid to either negative
627 or positive samples. From Table 5, it can be found when $\omega = "1"$ in dataset *Splitting No. 1*, two out of
628 fifteen defects escaped from the detection and one normal sample was mis-identified as abnormal. While
629 after applying the weighted binary cross entropy loss with weight $\omega = "0.1"$, the number of both false
630 negative and false positive decreased, which can be represented by the increased mean value and reduced

631 standard deviation after splitting the dataset, thus proving the effectiveness of the WCE loss function in
632 dealing with this imbalanced dataset issue.

633 **6.2.3 Selection of batch size**

634 Fixing the structure of network - the dilated CNN+GRU (32), and the loss weight $\omega = "0.1"$ for
635 training, we conducted controlled experiments to explore the effect of the training batch size on the model
636 performance. By setting the batch size as "4, 8" respectively as in Table 5, it was observed with gradual
637 improvement of the model in terms of averaged means and standard deviations of key performance
638 metrics, while the accuracy deviated in larger extent as the batch size further increased from "8" to "16".
639 Based on these findings, we trained our final proposed model with batch size as "8" to make a balance
640 between the training speed and the memory consumption. It should be noted that when batch size is
641 smaller than "8", such as "4", we randomly add one negative sample to each mini-batch, which means
642 that there would be "3" normal samples together with 1 abnormal sample in a mini-batch. When batch
643 size is equal or larger than "8", we followed the "1/8 portion" training strategy described in Section 6.2.

644 **6.2.4. Model compression**

645 In previous sections, we have verified the effectiveness of the dilated CNN+GRU framework in
646 solving the condition monitoring problem that we formulated in Section 3. It is valuable to explore the
647 optimal model configurations with leveraged efficiency and accuracy. Consequently, we made attempts
648 regarding the two main components of the network – the dilated CNN and the GRU respectively. To be
649 more specific, we first tried to halve the channel number of the last three dilated convolutional layers,
650 from (128, 256, 128) to (64, 128, 64). We then halved the number of neurons in GRU cell from "32" to
651 "16". The performance of the models has then been evaluated after splitting the dataset, the result of
652 which will be discussed in the next session.

653 **6.2.5. Model performance comparison after splitting dataset**

654 As mentioned, in order to thoroughly evaluate the robustness of the model in different compression
655 scenarios, we have split the training and evaluation sets for multiple times while testing on the identical
656 test set correspondingly. To systematically quantify the model performance under different parameter
657 configurations, we calculated the mean (μ) and standard deviation (σ) values for "Precision", "Recall"
658 and "F1-Score" values accordingly under five typically split dataset. As shown in Table 6, among the
659 three models as $M_1 = \text{Dilated CNN (256) + GRU (32)}$, $M_2 = \text{Dilated CNN (128) + GRU (32)}$ and $M_3 =$
660 $\text{Dilated CNN (256) + GRU (16)}$, the μ of M_1 achieved the largest value, indicating the model achieved
661 higher accuracy and precision for predicting the health status of elevator under both normal and abnormal
662 conditions. After comparing the standard deviation among the three models, it was found that the σ values
663 of M_1 also demonstrated the least variation among the three candidate models, thus showing the best
664 stability and robustness of this model.

665 **Table 4**
666 Performance of models with different architectures.

		Splitting	Confusion Matrix		Precision	Recall	F1-Score	Support	
<i>CNN+MLP</i>	0	<i>Abnormal</i>	13(TP)	2 (FN)	0.93	0.87	0.90	15	
		<i>Normal</i>	1 (FP)	1007(TN)	1.00	1.00	1.00	1008	
	1	<i>Abnormal</i>	13	2	0.81	0.87	0.84	15	
		<i>Normal</i>	3	1005	1.00	1.00	1.00	1008	
	4	<i>Abnormal</i>	14	1	1.00	0.93	0.97	15	
		<i>Normal</i>	0	1008	1.00	1.00	1.00	1008	
	5	<i>Abnormal</i>	10	5	0.77	0.67	0.71	15	
		<i>Normal</i>	3	1005	1.00	1.00	1.00	1008	
	9	<i>Abnormal</i>	12	3	0.86	0.80	0.83	15	
		<i>Normal</i>	2	1006	1.00	1.00	1.00	1008	
				<i>Ab. M. (μ)</i>	0.87	0.83	0.85		
				<i>Ab. S. (σ)</i>	0.09	0.10	0.10		
	<i>CNN+GRU</i>	0	<i>Abnormal</i>	13	2	1.00	0.87	0.93	15
			<i>Normal</i>	0	1008	1.00	1.00	1.00	1008
1		<i>Abnormal</i>	14	1	1.00	0.93	0.97	15	
		<i>Normal</i>	.0	1008	1.00	1.00	1.00	1008	
4		<i>Abnormal</i>	13	2	1.00	0.87	0.93	15	
		<i>Normal</i>	0	1008	1.00	1.00	1.00	1008	
5		<i>Abnormal</i>	14	1	1.00	0.93	0.97	15	
		<i>Normal</i>	0	1008	1.00	1.00	1.00	1008	
9		<i>Abnormal</i>	14	1	1.00	0.93	0.97	15	
		<i>Normal</i>	0	1008	1.00	1.00	1.00	1008	
			<i>Ab. M. (μ)</i>	1.00	0.91	0.95			
			<i>Ab. S. (σ)</i>	0	0.03	0.02			
<i>Dilated CNN+MLP</i>		0	<i>Abnormal</i>	14	1	0.82	0.93	0.87	15
			<i>Normal</i>	3	1005	1.00	1.00	1.00	1008
	1	<i>Abnormal</i>	11	4	0.73	0.73	0.73	15	
		<i>Normal</i>	4	1004	1.00	1.00	1.00	1008	
	4	<i>Abnormal</i>	14	1	0.88	0.93	0.90	15	
		<i>Normal</i>	2	1006	1.00	1.00	1.00	1008	
	5	<i>Abnormal</i>	15	0	0.79	1.00	0.88	15	
		<i>Normal</i>	4	1004	1.00	1.00	1.00	1008	
	9	<i>Abnormal</i>	12	3	0.71	0.80	0.75	15	
		<i>Normal</i>	5	1003	1.00	1.00	1.00	1008	
				<i>Ab. M. (μ)</i>	0.79	0.88	0.83		
				<i>Ab. S. (σ)</i>	0.07	0.11	0.08		
	<i>Dilated CNN+GRU</i>	0	<i>Abnormal</i>	14	1	1.00	0.93	0.97	15
			<i>Normal</i>	0	1008	1.00	1.00	1.00	1008
1		<i>Abnormal</i>	14	1	1.00	0.93	0.97	15	
		<i>Normal</i>	0	1008	1.00	1.00	1.00	1008	
4		<i>Abnormal</i>	14	1	1.00	0.93	0.97	15	
		<i>Normal</i>	0	1008	1.00	1.00	1.00	1008	
5		<i>Abnormal</i>	14	1	1.00	0.93	0.97	15	
		<i>Normal</i>	0	1008	1.00	1.00	1.00	1008	
9		<i>Abnormal</i>	14	1	1.00	0.93	0.97	15	
		<i>Normal</i>	0	1008	1.00	1.00	1.00	1008	
			<i>Ab. M. (μ)</i>	1.00	0.93	0.97			
			<i>Ab. S. (σ)</i>	0	0	0			

Note: 1). The GRU cell used here are of 32 neurons in the gate; 2). *Ab. M.* & *Ab. S.* represent the mean and standard deviation for fault detection under abnormal conditions.

667

668

669

670

671 **Table 5**
672 Performance of models with different training hyperparameters.

	(batch size, loss weight)	Splitting	Confusion matrix		Precision	Recall	F1-Score	Support			
<i>Dilate d CNN +GRU</i>	(4, 0.1)	0	<i>Abnormal</i>	14(TP)	1 (FN)	1.00	0.93	0.97	15		
			<i>Normal</i>	0 (FP)	1008(TN)	1.00	1.00	1.00	1008		
		1	<i>Abnormal</i>	15	0	1.00	1.00	1.00	15		
			<i>Normal</i>	0	1008	1.00	1.00	1.00	1008		
		4	<i>Abnormal</i>	14	1	1.00	0.93	0.97	15		
			<i>Normal</i>	0	1008	1.00	1.00	1.00	1008		
		5	<i>Abnormal</i>	15	0	0.06	1.00	0.11	15		
			<i>Normal</i>	237	771	1.00	0.76	0.87	1008		
		9	<i>Abnormal</i>	14	1	1.00	0.93	0.97	15		
			<i>Normal</i>	0	1008	1.00	1.00	1.00	1008		
							<i>Ab. M. (μ)</i>	0.81	0.96	0.80	
							<i>Ab. S. (σ)</i>	0.42	0	0	
	(16, 0.1)	0	<i>Abnormal</i>	14	1	1.00	0.93	0.97	15		
			<i>Normal</i>	0	1008	1.00	1.00	1.00	1008		
		1	<i>Abnormal</i>	14	1	0.93	0.93	0.93	15		
			<i>Normal</i>	1	1007	1.00	1.00	1.00	1008		
		4	<i>Abnormal</i>	13	2	1	0.87	0.93	15		
			<i>Normal</i>	0	1008	1.00	1.00	1.00	1008		
		5	<i>Abnormal</i>	14	1	0.93	0.93	0.93	15		
			<i>Normal</i>	1	1007	1.00	1.00	1.00	1008		
		9	<i>Abnormal</i>	15	0	0.83	1.00	0.91	15		
			<i>Normal</i>	3	1005	1.00	1.00	1.00	1008		
							<i>Ab. M. (μ)</i>	0.94	0.93	0.93	
							<i>Ab. S. (σ)</i>	0.07	0	0	
	(8, 1)	0	<i>Abnormal</i>	13	2	0.93	0.87	0.90	15		
			<i>Normal</i>	1	1007	1.00	1.00	1.00	1008		
		1	<i>Abnormal</i>	14	1	1.00	0.93	0.97	15		
			<i>Normal</i>	0	1008	1.00	1.00	1.00	1008		
		4	<i>Abnormal</i>	14	1	0.88	0.93	0.90	15		
			<i>Normal</i>	2	1006	1.00	1.00	1.00	1008		
5		<i>Abnormal</i>	14	1	0.93	0.93	0.93	15			
		<i>Normal</i>	1	1007	1.00	1.00	1.00	1008			
9		<i>Abnormal</i>	14	1	1.00	0.93	0.97	15			
		<i>Normal</i>	0	1008	1.00	1.00	1.00	1008			
					<i>Ab. M. (μ)</i>	0.95	0.92	0.93			
					<i>Ab. S. (σ)</i>	0.05	0	0			
(8, 0.1)	0	<i>Abnormal</i>	14	1	1	0.93	0.97	15			
		<i>Normal</i>	0	1008	1.00	1.00	1.00	1008			
	1	<i>Abnormal</i>	14	1	1	0.93	0.97	15			
		<i>Normal</i>	0	1008	1.00	1.00	1.00	1008			
	4	<i>Abnormal</i>	14	1	1	0.93	0.97	15			
		<i>Normal</i>	0	1008	1.00	1.00	1.00	1008			
	5	<i>Abnormal</i>	14	1	1	0.93	0.97	15			
		<i>Normal</i>	0	1008	1.00	1.00	1.00	1008			
	9	<i>Abnormal</i>	14	1	1	0.93	0.97	15			
		<i>Normal</i>	0	1008	1.00	1.00	1.00	1008			
						<i>Ab. M. (μ)</i>	1	0.93	0.97		
						<i>Ab. S. (σ)</i>	0	0	0		

Note: 1). The GRU cell used here are of 32 neurons in the gate; 2). *Ab. M.* & *Ab. S.* represent the mean and standard deviation for fault detection under abnormal conditions.

673

674

675

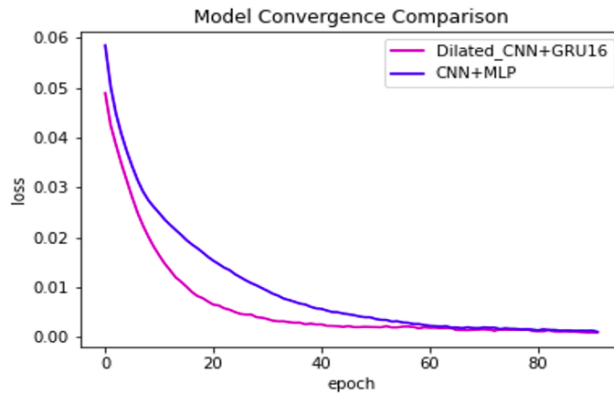
676 **Table 6**
677 Performance evaluation after compression with different model configurations.

Model Configuration	Splitting		Confusion Matrix		Precision	Recall	F1-Score	Support
M_1 = Dilated_CN	0	Abnormal	14(TP)	1 (FN)	1.00	0.93	0.97	15
		Normal	0 (FP)	1008(TN)	1.00	1.00	1.00	1008
N_256_GR	1	Abnormal	14	1	1.00	0.93	0.97	15
		Normal	0	1008	1.00	1.00	1.00	1008
U_32 (16, 128, 256, 128, 32)	4	Abnormal	14	1	1.00	0.93	0.97	15
		Normal	0	1008	1.00	1.00	1.00	1008
	5	Abnormal	14	1	1.00	0.93	0.97	15
		Normal	0	1008	1.00	1.00	1.00	1008
	9	Abnormal	14	1	1.00	0.93	0.97	15
		Normal	0	1008	1.00	1.00	1.00	1008
					<i>Ab. M. (μ)</i>	1.00	0.93	0.97
					<i>Ab. S. (σ)</i>	0	0	0
M_2 = Dilated CNN_128_ GRU_32	0	Abnormal	14	1	0.88	0.93	0.90	15
		Normal	2	1006	1.00	1.00	1.00	1008
(16, 64, 128, 64, 32)	1	Abnormal	14	1	0.82	0.93	0.87	15
		Normal	3	1005	1.00	1.00	1.00	1008
	4	Abnormal	14	1	0.93	0.93	0.93	15
		Normal	1	1007	1.00	1.00	1.00	1008
<i>Dilated CNN +GRU</i>	5	Abnormal	13	2	1.00	0.87	0.93	15
		Normal	0	1008	1.00	1.00	1.00	1008
	9	Abnormal	14	1	1.00	0.93	0.97	15
		Normal	0	1008	1.00	1.00	1.00	1008
					<i>Ab. M. (μ)</i>	0.93	0.92	0.92
					<i>Ab. S. (σ)</i>	0.08	0.03	0.04
M_3 = Dilated_CN	0	Abnormal	14	1	1.00	0.93	0.97	15
		Normal	0	1008	1.00	1.00	1.00	1008
N_256_GR	1	Abnormal	13	2	1.00	0.87	0.93	15
		Normal	0	1008	1.00	1.00	1.00	1008
U_16 (16, 128, 256, 128, 16)	4	Abnormal	13	2	0.93	0.87	0.90	15
		Normal	1	1007	1.00	1.00	1.00	1008
	5	Abnormal	15	0	1.00	1.00	1.00	15
		Normal	0	1008	1.00	1.00	1.00	1008
	9	Abnormal	14	1	1.00	0.93	0.97	15
		Normal	0	1008	1.00	1.00	1.00	1008
					<i>Ab. M. (μ)</i>	0.99	0.92	0.95
					<i>Ab. S. (σ)</i>	0.03	0.05	0.04

Note: 1). Parameters (a,b,c,d,e) in the column of Model configuration represent the number of filters for the four convolutional layers and the number of neurons in the gate of GRU cell; 2). Ab. M. & Ab. S. represent the mean and standard deviation for fault detection under abnormal conditions.

678
679 It was thus concluded that the more complex the model, the more robust and stable the model
680 appeared in the mentioned dataset for different configuration scenarios. Under the case of M_3 , though
681 the larger σ value was witnessed while representing larger performance deviations in comparison with
682 M_1 , whereas the *mean value* of precision metric ($\mu=0.99$) almost scored the same high with $M_1(\mu=1.00)$.
683 Consequently, considering the demand with real-case applications of the proposed DL model into the lift
684 sites in normal operation, the streamlined architecture (in M_3) would help boost the inferencing and
685 computational speed under leaner architectures. Hence, considering the minor difference in accuracy
686 performance deviations, together with the higher demand for robustness on the elevator sites, we would
687 choose M_3 = Dilated CNN (256) + GRU (16) as the appropriate model for practical application.

688
689
690
691
692
693
694



695 **Fig. 11.** Comparison of loss reduction speed and convergence performance.

696 **6.2.6. Model efficiency and convergence performance**

697 Regarding the model efficiency, it was proved that the quantity of parameters were reduced by 21%
698 from around “268K” to “211K” for the proposed Dilated CNN+GRU (16) in comparison with the vanilla
699 CNN+MLP model, thus largely improving the model performance with lessened computation
700 complexity and lightweight architecture. Meanwhile, the receptive field was also enlarged by “75%”
701 from the original (126×32) in the vanilla CNN+MLP structure to the current (220×32) under the optimal
702 architecture with the Dilated CNN+GRU (16) model. Regarding the model convergence performance
703 during the training process, it could be validated by Fig. 11 that the proposed Dilated CNN+GRU (16)
704 model demonstrated comparatively faster convergence speed under fewer epochs’ iteration in terms of
705 loss reduction compared with the vanilla CNN+MLP model. Consequently, the optimal model of Dilated
706 CNN+GRU (16) was derived with more lightweight architecture and enhanced efficiency in simplicity
707 and elegance.

708 The model effectiveness could be validated by the following perspectives, on the one hand, by
709 replacing the vanilla convolutional layer in the backbone with dilated convolutional layer, the receptive
710 field was expanded dramatically with fewer parameters; on the other hand, the concatenation of GRU
711 layer instead of the trivial MLP could enhance the temporal correlation among the extracted feature
712 representations to enhance the overall efficiency.

713 By specifying model structure as the Dilated CNN+GRU (16) and setting batch size equal to “8” with
714 loss weight as “0.1” in the weighted cross-entropy loss, the testing results were leveraged among the best
715 evaluation matrix outcomes, which demonstrated the superior performance of the proposed model.
716 Meanwhile, the core metrics of precision, recall and F1-Score for normal conditions also reached “1.00”
717 with good capability in recognizing and distinguishing the normal situations during elevator condition
718 monitoring. Furthermore, the anomaly detector conducted the role of the classifier with the optimal
719 threshold learned through the training process to determine the elevator status.

720

721 7. Managerial implications

722 The routine safety surveillance on elevators during the practical operation process proves to be a
723 crucial topic for corporate managerial and executive personnel in relevant elevator manufacturers and
724 maintenance-responsible enterprises. By the prevailing measures taken for anomaly detection on
725 elevator's electrical and mechanical (E&M) systems, the most commonly used post-hoc routine
726 inspection manner would inevitably cause unexpected delays for detecting the faults with gradual
727 degradation of safety-critical components. Moreover, such conventional methods are mostly restricted
728 by the proprietary intrusive equipment while lacking applicability on elevators of different brands in a
729 broad scope. With the emerging artificial intelligence technology, under a wide plethora of research
730 utilizing data-driven methods for condition monitoring, it has been recognized as a critical topic to tackle
731 the influence of the imbalanced dataset issue. Especially for deep learning-based data-driven approaches,
732 the imbalanced dataset would cause the inadequate extraction of multi-level and cross-hierarchical
733 feature dependencies, while leading to the insufficient learning of data characteristics with suboptimal
734 fault detection accuracy. Though there exist devious workaround routes such as the data manipulation
735 with laboratory synthetic experiments, or the stacking of complicated deep learning model architectures
736 trying to increase the complexity of models with the presumably better feature learning capabilities, the
737 side effects could not be neglected as well while impairing the monitoring effectiveness. For instance,
738 laboratory synthetic data manipulation would lead to the real data generated in the highly dynamic actual
739 elevator operation conditions not being captured and learnt, while decreasing the model's generalization
740 capability during practical deployment; whilst the complexity increasement would also lead to excessive
741 model parameters as generated, thus affecting the model's inferencing speed and computation efficiency.
742 Especially for real deployment to actual elevator operation sites, much greater demands are put forward
743 to the proposed solutions with streamlined lean architectures without excessive computation power
744 consumption while handling a wide variety of real-case imbalanced dataset issues with good
745 generalization capability. Hence, a delicate balance point might be required for the proposed feasible
746 solutions customized for real-case applications to the elevator condition monitoring domain.

747 Anchored in the practical requirement as mentioned above, this paper proposes a novel deep learning
748 model with a lightweight architecture without adding excessive computation burdens, while the devised
749 training strategy and other embedded algorithmic designs could effectively alleviate the impacts of
750 imbalanced dataset as well during the actual implementation process. There are a couple of manifold
751 implications for the managerial level of enterprise from the following perspectives by the proposed work:

752 1). *Innovative Monitoring Manner.* Distinct from the conventional prevailing measure with routine
753 site inspection and maintenance on specific components using proprietary equipment, the proposed
754 solution was established based on a non-invasive framework while monitoring the electric current signals
755 flowing through the core components, namely the traction motor, brake system, safety circuit and lift
756 door. By observing the patterns of electric current signals, the health condition of the critical safety-

757 relevant components can be monitored remotely with anomaly detection performed by the proposed deep
758 learning model. Whilst the data are collected via Internet-of-Things (IoT) sensors and transferred via a
759 Cloud-based data hub with constant surveillance on the functionality of elevators. Such innovative
760 monitoring manner with the adoption of IoT sensors and AI deep learning analytical models can provide
761 an efficient smart way of monitoring in comparison with conventional methods, while eliminating the
762 cumbersome efforts of onsite regular checking and post-hoc maintenance after the occurrence of elevator
763 accidents, thus improving the overall safety level of elevators in routine operations.

764 *2). Enhanced Feature Extraction Capability.* The proposed model can enhance the temporal feature
765 correlations by the devised gated recurrent unit (GRU) architecture, especially capable of learning the
766 multi-scale and cross-hierarchical timeseries data patterns. Due to the electric current signals are
767 collected constantly under high sampling rates by the IoT sensors, hence the temporal feature correlations
768 play a decisive role in analysing the multi-channel current signals for fault detection. Meanwhile, the
769 proposed model has concatenated the dilated convolutional neural network (DiCNN), while largely
770 increasing the receptive fields by 75% in comparison with the state-of-the-art baseline model, thus
771 stimulating the neuronal response with evoked feature correlations and enhanced learning effectiveness
772 on the multi-variant data characteristics.

773 *3). Improved Inferencing Speed.* By the experimental validation, it is proved that the proposed Dilated
774 CNN+GRU (16) model demonstrated comparatively faster convergence speed under fewer epochs'
775 iteration in terms of loss reduction compared with the vanilla CNN+MLP baseline model. Such
776 performance factors as emphasized by the managerial level of companies could affect the model's
777 training efficiency and inference speed with positive correlations. For elevators installed under the highly
778 dynamic real operational environment, the improved training and inference speed shall be a crucial
779 evaluation point for managers while considering the applicability of the proposed model to cater the real-
780 time elevator monitoring circumstances.

781 *4). Model Elegancy with Non-excessive Complexity.* By the proposed model, the parameter quantity
782 has been dramatically reduced by 21% in comparison with the CNN+MLP baseline model. Rather than
783 stacking the complex deep learning architectures, the proposed lightweight model presents a streamlined
784 architecture with largely reduced model parameters, which could provide a useful implication for
785 managerial level in selection of the appropriate models with reduced complexity and enhanced efficiency.

786 *5). Delicate Balance Between Model Efficiency and Ingenious Imbalanced Dataset Tackling Methods.*
787 There exist various methods for alleviating the impacts of the imbalanced dataset issue, yet could be
788 overshadowed with inferior performance against the complex dataset as composed of the elevator's real-
789 operational heterogeneous electric current signal data. Alternatively, the laboratory synthesis of minority
790 class samples would impair the model's generalization capability, whilst the stacking of complicated
791 redundant model structures in remedy of the insufficient minority-class feature learning could affect the

792 model's inferencing speed during actual deployment. Hence, under the real-case high demands for real-
793 time monitoring, how to delicately implement a feasible way for tackling the imbalanced dataset issue
794 while retaining the model's structural elegance without adding additional computation burdens could be
795 one of the top concerns for managerial levels. By the proposed devised training strategy and customized
796 loss function, the model has achieved superior performance with the high precision value after the
797 systematic ablation studies, thus justifying the effectiveness of the proposed methods for addressing and
798 alleviating the imbalanced dataset issue for elevator condition monitoring based on the real-collected
799 dataset during the actual elevator operation process.

800 For the corporate managers or investors in elevator manufacturing or maintenance responsible
801 enterprises, all the aforementioned implications could be taken into consideration to support their
802 strategic decision-making while aiming to construct the holistic non-intrusive elevator monitoring
803 framework during the digital transformation process. On the one hand, this paper provides one of the
804 pioneering works for utilizing the deep learning-based data-driven models in the domain of non-intrusive
805 elevator condition monitoring, the framework of which brings considerable reference value for
806 managerial-level personnel in such companies. On the other hand, this paper proposes a relatively lean
807 architectural framework in adoption of the streamlined deep learning model with reduced parameters and
808 enhanced feature extraction capability to boost the lean digitalization (Zhang et al., 2025) for such
809 companies, while laying a solid foundation to facilitate further in-depth research and application in
810 relevant domains. Moreover, the proposed model is customized with wide applicability using real-case
811 elevator operation data and feasible measures to tackle the imbalanced dataset issue, thus largely
812 enhancing the model's generalization capability during the practical commissioning process by the
813 managerial-level personnel. Consequently, the work proposed in this paper has brought manifold
814 managerial implications from different perspectives and paved the way for constructing the AI-
815 empowered smart elevator monitoring framework with advanced engineering management technologies
816 for broad practical applications.

817 **8. Conclusions**

818 This paper has proposed a novel deep learning-based solution for the condition monitoring and
819 anomaly detection of elevators under imbalanced dataset to foster practical applications with diversified
820 environmental dynamics. With the model architecture composing the customised Dilated CNN and GRU
821 under the explored optimal configurations through the ablation study, the proposed 1D-DiCNN-GRU
822 model demonstrated supreme robustness and accuracy in fault detection by analysing the elevator's
823 electric current signals as non-intrusively captured in real life. The proposed solution generated the
824 optimum performance to tackle the industrial bottleneck under imbalanced dataset scenarios with a
825 relatively lightweight but elegant architecture while capturing both the intricate spatial and temporal data

826 correlations from multi-variant time-series 1D signals directly, so as to seek broader applications by
827 industrial practitioners.

828 Expect for the research rigour evaluation via the devised testing scenarios and systematic ablation
829 studies, the model's robustness was also validated through real practice by field experts in the elevator
830 industry. As an effective supplementary system to the prevailing conventional lift monitoring
831 mechanisms, the proposed model and system can provide a rather convenient retrofitting method by non-
832 intrusively installing the clamp-type electric current sensors with embedded AI algorithms for routine
833 elevator status monitoring. Such a smart approach can help industrial practitioners effectively measure
834 the degradation status of elevators with relatively simple but elegant model architecture to propel the
835 utilization of AI technology in safety-critical systems, which can increase their efficiency with the
836 integrated capability for predictive maintenance.

837 As well acknowledged that the collection of abnormal signals proves very challenging and laborious
838 in real life. Deemed as one of the major contributions, we also established an industrial dataset based on
839 the non-invasive signals as captured and measured during the real observation process for lift condition
840 monitoring. Regarding future improvement, a more robust algorithmic mechanism to tackle the
841 imbalanced dataset issue shall be explored and refined, while facilitating the construction of a more
842 rigorous dataset architecture with enhanced integrity for real-life data observation. More advanced data-
843 driven analytical model by integrating with state-of-the-art DL methodologies shall be further
844 investigated and validated to leverage the sustainability of model performance with more accurate
845 anomaly detection and fault diagnosis results.

846

847 **Acknowledgements**

848 The work presented in this paper is supported by Centre for Advances in Reliability and Safety
849 (CAiRS) admitted under AIR@InnoHK Research Cluster. Real-world electric current data on the
850 elevator system provided by a CAiRS partner is also acknowledged. This paper also contributes to the
851 PhD thesis of author Ye Wang for acknowledgement.

852

853

854

855

856

857

- 859 Aheleroff, S., Xu, X., Lu, Y., Aristizabal, M., Pablo Velásquez, J., Joa, B., & Valencia, Y. (2020). IoT-enabled
860 smart appliances under industry 4.0: A case study. *Advanced Engineering Informatics*, 43, 101043.
- 861 Analide, C., Novais, P., Camacho, D., & Yin, H. (2020). A Preprocessing Approach for Class-Imbalanced Data
862 Using SMOTE and Belief Function Theory. In (Vol. 12490). Springer International Publishing AG.
- 863 Arora, V., Yin-Kwee Ng, E., & Singh, A. (2022). Chapter One - Machine learning and its applications. In R. Sehgal,
864 N. Gupta, A. Tomar, M. D. Sharma, & V. Kumaran (Eds.), *Smart Electrical and Mechanical Systems* (pp.
865 1-37). Academic Press.
- 866 Bisong, E. (2019). *Building Machine Learning and Deep Learning Models on Google Cloud Platform: A*
867 *Comprehensive Guide for Beginners*. Apress L. P.
- 868 Chai, S., Li, X. L., Jia, Y., He, Y., Yip, C. H., Cheung, K. K., & Wang, M. (2021). A Non-Intrusive Deep Learning
869 Based Diagnosis System for Elevators. *IEEE Access*, 9, 20993-21003.
- 870 Chen, Z., Guo, R., Lin, Z., Peng, T., & Peng, X. (2021). A Data-Driven Health Monitoring Method Using
871 Multiobjective Optimization and Stacked Autoencoder Based Health Indicator. *IEEE Transactions on*
872 *Industrial Informatics*, 17(9), 6379-6389.
- 873 Chung, J., Gulcehre, C., Cho, K., & Bengio, Y. (2014, December 2014). Empirical evaluation of gated recurrent
874 neural networks on sequence modeling. NIPS 2014 Workshop on Deep Learning,
- 875 Dai, X., & Gao, Z. (2013). From Model, Signal to Knowledge: A Data-Driven Perspective of Fault Detection and
876 Diagnosis. *IEEE Transactions on Industrial Informatics*, 9(4), 2226-2238.
- 877 de Oliveira, J. P. G., J.A. Bastos-Filho, C., & Oliveira, S. C. (2022). Non-invasive embedded system
878 hardware/firmware anomaly detection based on the electric current signature. *Advanced Engineering*
879 *Informatics*, 51, 101519.
- 880 Dong, Y., & Wang, X. (2011). A New Over-Sampling Approach: Random-SMOTE for Learning from Imbalanced
881 Data Sets. Berlin, Heidelberg.
- 882 Douzas, G., & Bacao, F. (2019). Geometric SMOTE a geometrically enhanced drop-in replacement for SMOTE.
883 *Information sciences*, 501, 118-135.
- 884 EMSD. (2022a). *Code of Practice on the Design and Construction of Lifts and Escalators*. Retrieved from
885 https://www.emsd.gov.hk/en/lifts_and_escalators_safety/publications/code_of_practice/index.html
- 886 EMSD. (2022b). *Lifts and Escalators Ordinance (Cap. 618)*.
887 https://www.elegislation.gov.hk/hk/cap618?tab=m&xpid=ID_1438403530602_001
- 888 EMSD. (2022c). *The summaries of the reported lift incidents*.
889 [https://www.emsd.gov.hk/en/lifts_and_escalators_safety/publications/contractors_performance_rating/r](https://www.emsd.gov.hk/en/lifts_and_escalators_safety/publications/contractors_performance_rating/reported_lift_incident_records/)
890 [eported_lift_incident_records/](https://www.emsd.gov.hk/en/lifts_and_escalators_safety/publications/contractors_performance_rating/reported_lift_incident_records/)
- 891 Esteban, E., Salgado, O., Iturrospe, A., & Isasa, I. (2014). Model-based estimation of elevator rail friction forces.
892 International Conference on Condition Monitoring of Machinery in Non-Stationary Operation,
- 893 Fang, W., Shao, Y., Love, P. E. D., Hartmann, T., & Liu, W. (2023). Detecting anomalies and de-noising monitoring
894 data from sensors: A smart data approach. *Advanced Engineering Informatics*, 55, 101870.
- 895 Feng, J., Yao, Y., Lu, S., & Liu, Y. (2021). Domain Knowledge-Based Deep-Broad Learning Framework for Fault
896 Diagnosis. *IEEE transactions on industrial electronics (1982)*, 68(4), 3454-3464.
- 897 Fu, Y., Liu, X., Sarkar, S., & Wu, T. (2021). Gaussian mixture model with feature selection: An embedded
898 approach. *Computers & Industrial Engineering*, 152, 107000.
- 899 Gao, Y., Zhang, H., Ding, L., Zhang, S., & Zeng, C. (2025). Overcoming the Digital Dilemmas: How Do
900 Enterprises Develop Digital Transformative Capability? *IEEE Transactions on Engineering*
901 *Management*, 72, 1653-1667.
- 902 García, Á., Bregon, A., & Martínez-Prieto, M. A. (2022). A non-intrusive Industry 4.0 retrofitting approach for
903 collaborative maintenance in traditional manufacturing. *Computers & Industrial Engineering*, 164,
904 107896.
- 905 Giovanni, P. D., Belvedere, V., & Grando, A. (2024). The Selection of Industry 4.0 Technologies Through
906 Bayesian Networks: An Operational Perspective. *IEEE Transactions on Engineering Management*, 71,
907 2921-2936.
- 908 González, M., Salgado, O., Hernandez, X., Croes, J., Pluymers, B., & Desmet, W. (2019). Model-based condition
909 monitoring of guiding rails in electro-mechanical systems. *Mechanical Systems and Signal Processing*,
910 120, 630-641.
- 911 Haibo, H., Yang, B., Garcia, E. A., & Shutao, L. (2008, 2008). ADASYN: Adaptive synthetic sampling approach
912 for imbalanced learning.
- 913 Hennig, M., Grafinger, M., Hofmann, R., Gerhard, D., Dumss, S., & Rosenberger, P. (2021). Introduction of a
914 time series machine learning methodology for the application in a production system. *Advanced*
915 *Engineering Informatics*, 47, 101197.

- 916 Huo, Y., Gu, Q., Cai, Z., & Yuan, L. (2015). Classification method for imbalance dataset based on genetic
917 algorithm improved synthetic minority over-sampling technique. *Jisuanji Yingyong / Journal of*
918 *Computer Applications*, 35(1), 121-139.
- 919 Ilango, H. S., Ma, M., & Su, R. (2022). A FeedForward–Convolutional Neural Network to Detect Low-Rate DoS
920 in IoT. *Engineering Applications of Artificial Intelligence*, 114, 105059.
- 921 Jaenal, A., Ruiz-Sarmiento, J.-R., & Gonzalez-Jimenez, J. (2024). MachNet, a general Deep Learning architecture
922 for Predictive Maintenance within the industry 4.0 paradigm. *Engineering Applications of Artificial*
923 *Intelligence*, 127, 107365.
- 924 Khan, A. Q., El Jaouhari, S., Tamani, N., & Mroueh, L. (2024). Knowledge-based anomaly detection: Survey,
925 challenges, and future directions. *Engineering Applications of Artificial Intelligence*, 136, 108996.
- 926 Koltun, F. Y. V. (2016, 30 Apr 2016). *Multi-scale Context Aggregation by Dilated Convolutions* International
927 Conference on Learning Representations,
- 928 Koutsoupakis, J., Giagopoulos, D., & Chatziparasidis, I. (2023). AI-based condition monitoring on mechanical
929 systems using multibody dynamics models. *Engineering Applications of Artificial Intelligence*, 123,
930 106467.
- 931 Kumar Sharma, D., Brahmachari, S., Singhal, K., & Gupta, D. (2022). Data driven predictive maintenance
932 applications for industrial systems with temporal convolutional networks. *Computers & Industrial*
933 *Engineering*, 169, 108213.
- 934 Lakemond, N., Holmberg, G., & Pettersson, A. (2024). Digital Transformation in Complex Systems. *IEEE*
935 *Transactions on Engineering Management*, 71, 192-204.
- 936 Li, H., Cao, P., Wang, X., Yi, B., Huang, M., Sun, Q., & Zhang, Y. (2023). Multi-task spatio-temporal augmented
937 net for industry equipment remaining useful life prediction. *Advanced Engineering Informatics*, 55,
938 101898.
- 939 Lin, Z., Duan, D., Yang, Q., Cheng, X., Yang, L., & Cui, S. (2018, 26-29 Nov. 2018). One-class Classifier Based
940 Fault Detection in Distribution Systems with Distributed Energy Resources. 2018 IEEE Global
941 Conference on Signal and Information Processing (GlobalSIP),
- 942 Lingxiao, Q., Ximing, Y., Yi, W., & Jin, C. (2025). Deciphering AI's Role in Corporate Innovation: A Holistic
943 Framework of AI Resources, Capability, and Performance. *IEEE Engineering Management Review*,
944 53(2), 85-95.
- 945 Liu, C., Zhang, X., Liu, X., & Chen, C. (2017). The research of elevator health diagnosis method based on
946 Bayesian network. IOP Conference Series: Earth and Environmental Science,
- 947 Liu, Y., Chen, H., Wang, Y., & Zhang, P. (2021). Power pooling: An adaptive pooling function for weakly labelled
948 sound event detection. 2021 International Joint Conference on Neural Networks (IJCNN),
- 949 Mahadevan, S., & Shah, S. (2009). Fault Detection and Diagnosis in Process Data Using One-Class Support
950 Vector Machines. *Journal of Process Control*, 19, 1627-1639.
- 951 Mazzoleni, M., Sarda, K., Acernese, A., Russo, L., Manfredi, L., Glielmo, L., & Del Vecchio, C. (2022). A fuzzy
952 logic-based approach for fault diagnosis and condition monitoring of industry 4.0 manufacturing
953 processes. *Engineering Applications of Artificial Intelligence*, 115, 105317.
- 954 Medghalchi, B., & Vogel, A. (2024). A machine learning-based algorithm for automated detection of frequency-
955 based events in recorded time series of sensor data. *Engineering Applications of Artificial Intelligence*,
956 133, 108536.
- 957 Mishra, K. M., & Huhtala, K. (2019). Elevator Fault Detection Using Profile Extraction and Deep Autoencoder
958 Feature Extraction for Acceleration and Magnetic Signals. *Applied Sciences*, 9(15).
- 959 Moura, J., Batista, F., Cardoso, E., & Nunes, L. (2019). Intelligent management and efficient operation of Big
960 Data. In *Web Services: Concepts, Methodologies, Tools, and Applications* (pp. 1991-2016). IGI Global.
- 961 Nguyen, T. N., Ngo, Q.-D., Nguyen, H.-T., & Giang, N. L. (2022). An Advanced Computing Approach for IoT-
962 Botnet Detection in Industrial Internet of Things. *IEEE Transactions on Industrial Informatics*, 1-1.
- 963 Rajnoha, R., & Hadač, J. (2024). Strategic Key Elements in Big Data Analytics as Driving Forces of IoT
964 Manufacturing Value Creation: A Challenge for Research Framework. *IEEE Transactions on*
965 *Engineering Management*, 71, 90-105.
- 966 Skog, I., Karagiannis, I., Bergsten, A. B., Harden, J., Gustafsson, L., & Handel, P. (2017). A Smart Sensor Node
967 for the Internet-of-Elevators—Non-Invasive Condition and Fault Monitoring. *IEEE Sensors Journal*,
968 17(16), 5198-5208.
- 969 Tang, J., Liu, Y., Lin, K.-y., & Li, L. (2023). Process bottlenecks identification and its root cause analysis using
970 fusion-based clustering and knowledge graph. *Advanced Engineering Informatics*, 55, 101862.
- 971 Tomczak, J. M. (2024). *Deep Generative Modeling* (1 ed.). Springer International Publishing AG.
- 972 Wan, Z., Yi, S., Li, K., Tao, R., Gou, M., Li, X., & Guo, S. (2015). Diagnosis of Elevator Faults with LS-SVM
973 Based on Optimization by K-CV. *Journal of Electrical and Computer Engineering*, 2015, 1-8.
- 974 Wang, J., Lim, M. K., Wang, C., & Tseng, M.-L. (2021). The evolution of the Internet of Things (IoT) over the
975 past 20 years. *Computers & Industrial Engineering*, 155, 107174.

976 Wen, P., Zhi, M., Zhang, G., & Li, S. (2016). Fault Prediction of Elevator Door System Based on PSO-BP Neural
977 Network. *Engineering*, 08(11), 761-766.

978 Wileman, A., Perinpanayagam, S., & Aslam, S. (2021). Physics of Failure (PoF) Based Lifetime Prediction of
979 Power Electronics at the Printed Circuit Board Level. *Applied Sciences*, 11(6).

980 Xiahou, T., Zeng, Z., & Liu, Y. (2021). Remaining Useful Life Prediction by Fusing Expert Knowledge and
981 Condition Monitoring Information. *IEEE Transactions on Industrial Informatics*, 17(4), 2653-2663.

982 Xu, C., & Lin, B. (2025). Embracing Artificial Intelligence: How Does Intelligent Transformation Affect the
983 Technological Innovation of New Energy Enterprises? *IEEE Transactions on Engineering Management*,
984 72, 703-716.

985 Xu, X., Li, X., Ming, W., & Chen, M. (2022). A novel multi-scale CNN and attention mechanism method with
986 multi-sensor signal for remaining useful life prediction. *Computers & Industrial Engineering*, 169,
987 108204.

988 Yan, J., He, Z., & He, S. (2022). A deep learning framework for sensor-equipped machine health indicator
989 construction and remaining useful life prediction. *Computers & Industrial Engineering*, 172, 108559.

990 Yin, S., Ding, S. X., Xie, X., & Luo, H. (2014). A Review on Basic Data-Driven Approaches for Industrial Process
991 Monitoring. *IEEE Transactions on Industrial Electronics*, 61(11), 6418-6428.

992 Yu, Y., Lakemond, N., & Holmberg, G. (2024). AI in the Context of Complex Intelligent Systems: Engineering
993 Management Consequences. *IEEE Transactions on Engineering Management*, 71, 6512-6525.

994 Zeng, Z., Kang, R., & Chen, Y. (2016). Using PoF models to predict system reliability considering failure
995 collaboration. *Chinese journal of aeronautics*, 29(5), 1294-1301.

996 Zhang, S., Bi, X., Tian, R., Chen, T., Ding, K., & Yu, Z. (2025). Lean Digitalization Solutions for SMEs in China.
997 *IEEE Transactions on Engineering Management*, 72, 1546-1558.

998 Zhou, Z., Huang, H., & Fang, B. (2021). Application of Weighted Cross-Entropy Loss Function in Intrusion
999 Detection. *Journal of Computer and Communications*, 09(11), 1-21.